Gael Forget
MIT, Jan. 16th 2015

Introduction to ocean data-model analysis

course 3 : model-data synthesis

1. fitting dynamics to data (interp., invers.)
2. theory and practice (least sq., opt. control)
3. ECCO v4 state estimate (data, model errors)
4. extended model-data analyses

5. interactive session : self-guided exercises
6. resources, bibliography

… course 4 : the global MITgcm setup

(1) Fitting Dynamics to Data

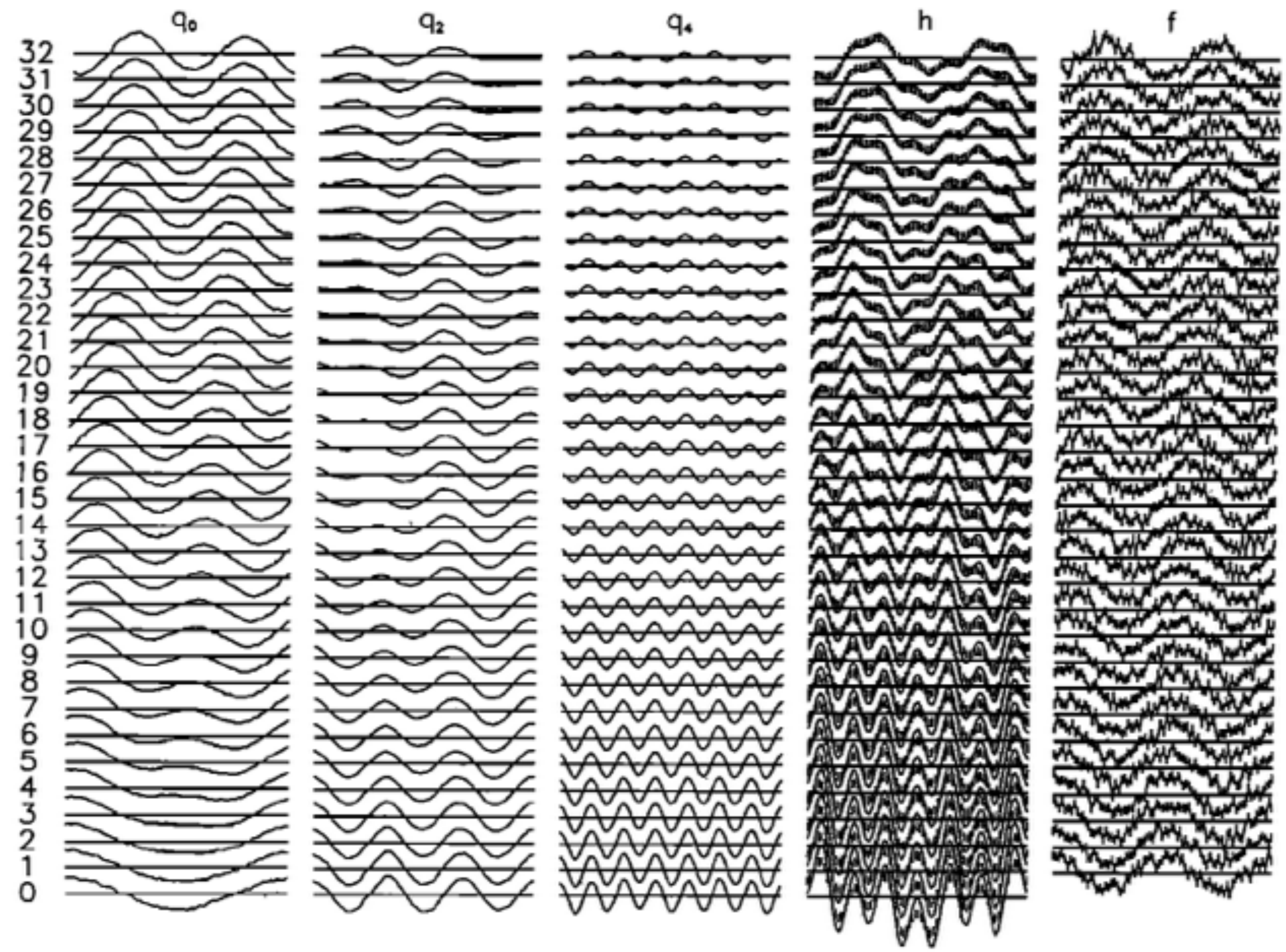

Fig. 6. Identical twin surface elevation data and noisy wind stress data are available everywhere at all times.

This case illustrates that highly accurate oceanographic data can in principle help in removing noise from wind observations. As for the previous case, the necessary quantity of oceanographic data are not likely to be available. Also for this

(1) Fitting Dynamics to Data

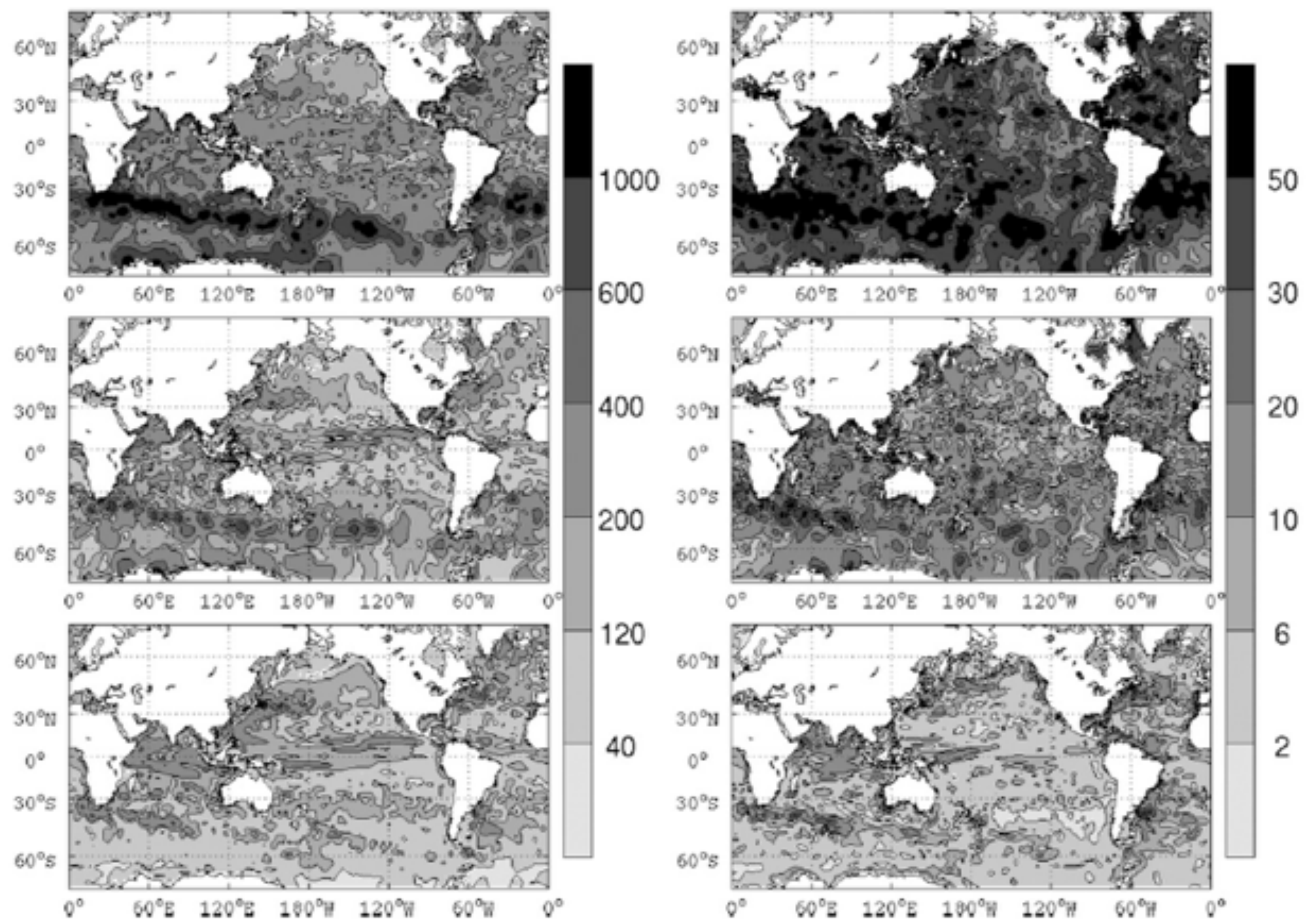

FIG. 14. Magnitude of the flux divergence fluctuation that is implied by the seasonal cycle of the vertically integrated (left) heat (W m^{-2}) and (right) freshwater (mm day^{-1}) content, for (top) *WOA01*, (middle) Fourier truncated *WOA01* (see appendix A), and (bottom) OCCA. The implied fluxes diagnostic computation is $\|\Delta\mathcal{H}/\Delta t\|$, where $\Delta\mathcal{H}$ is the content difference from one month to the next, Δt is one month, and double vertical bars stand for standard deviation of mean monthly values. Note that such diagnostics do not reflect annual mean fluxes, but only the seasonal fluctuation. Contents of T and S are converted to heat and freshwater units by multiplication with $\rho \times C_p = 4000 \times 1000$ or $1/S_0 = 1/35$, respectively.

Dynamical constraints: a means to filter 'noise'

(1) Fitting Dynamics to Data

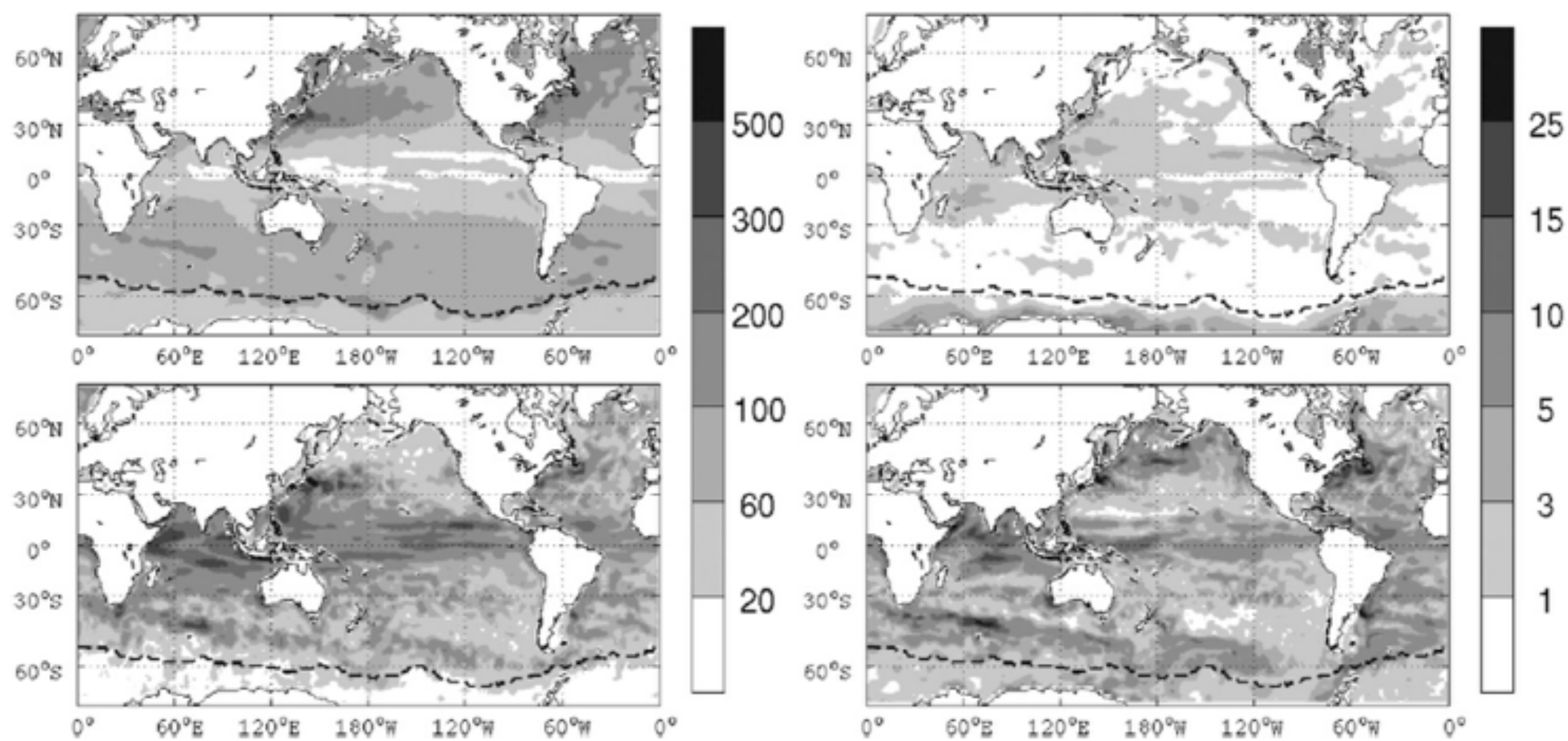

FIG. 16. Amplitude of the fluxes that contribute to the seasonal cycle of the vertically integrated (left) heat (W m^{-2}) and (right) freshwater (mm day^{-1}) content in OCCA. (top) Part due to fluxes through the ocean surface ($\|\mathcal{S}\|$) that consist of air–sea fluxes, ice–sea fluxes, and runoff. The dashed line demarcates the region that experiences sea ice coverage, where $\|\mathcal{S}\|$ largely consists of ice–sea fluxes due to the sea ice coverage seasonal fluctuation. (bottom) Part due to the divergence of fluxes within the ocean ($\|\mathcal{O}\|$) that consist of advection and mixing. Brackets stand for standard deviation of mean monthly values, which implies that annual mean fluxes are omitted (like Fig. 14, but unlike Fig. 13). These fields may be compared with those in Fig. 14 that show inferences of $\|\mathcal{T}\| = \|\mathcal{S}+\mathcal{O}\|$.

State Estimate: a dynamical interpretation of the data

(1) Fitting Dynamics to Data

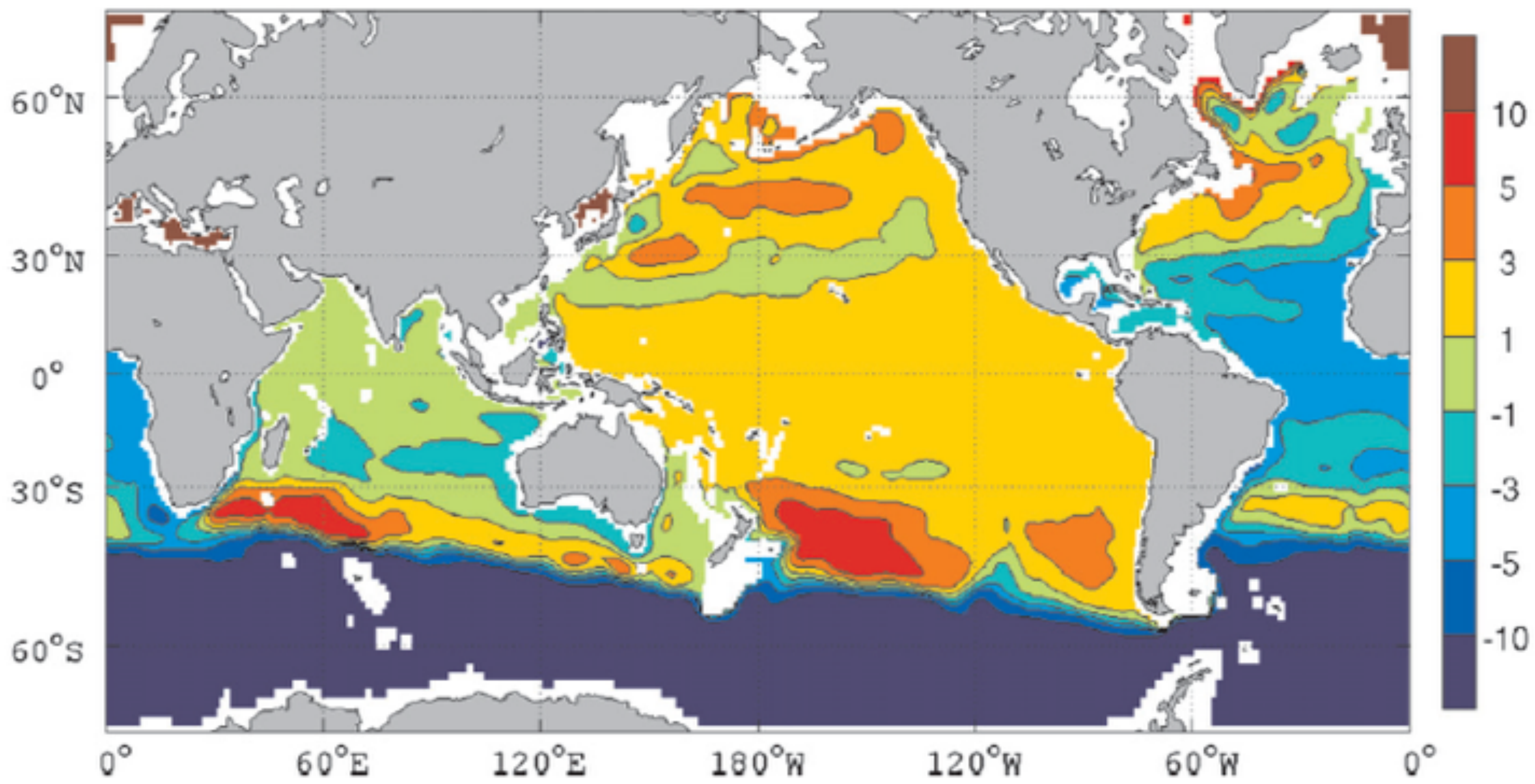

FIG. 10. Annual mean dynamic topography (cm) at 1600-m depth in OCCA. This quantity is the pressure anomaly at 1600 m expressed in cm. Regions that are not color shaded are those where the sea floor is above 1600 m.

Adjoint model: **a means to combine data types**

(1) Fitting Dynamics to Data

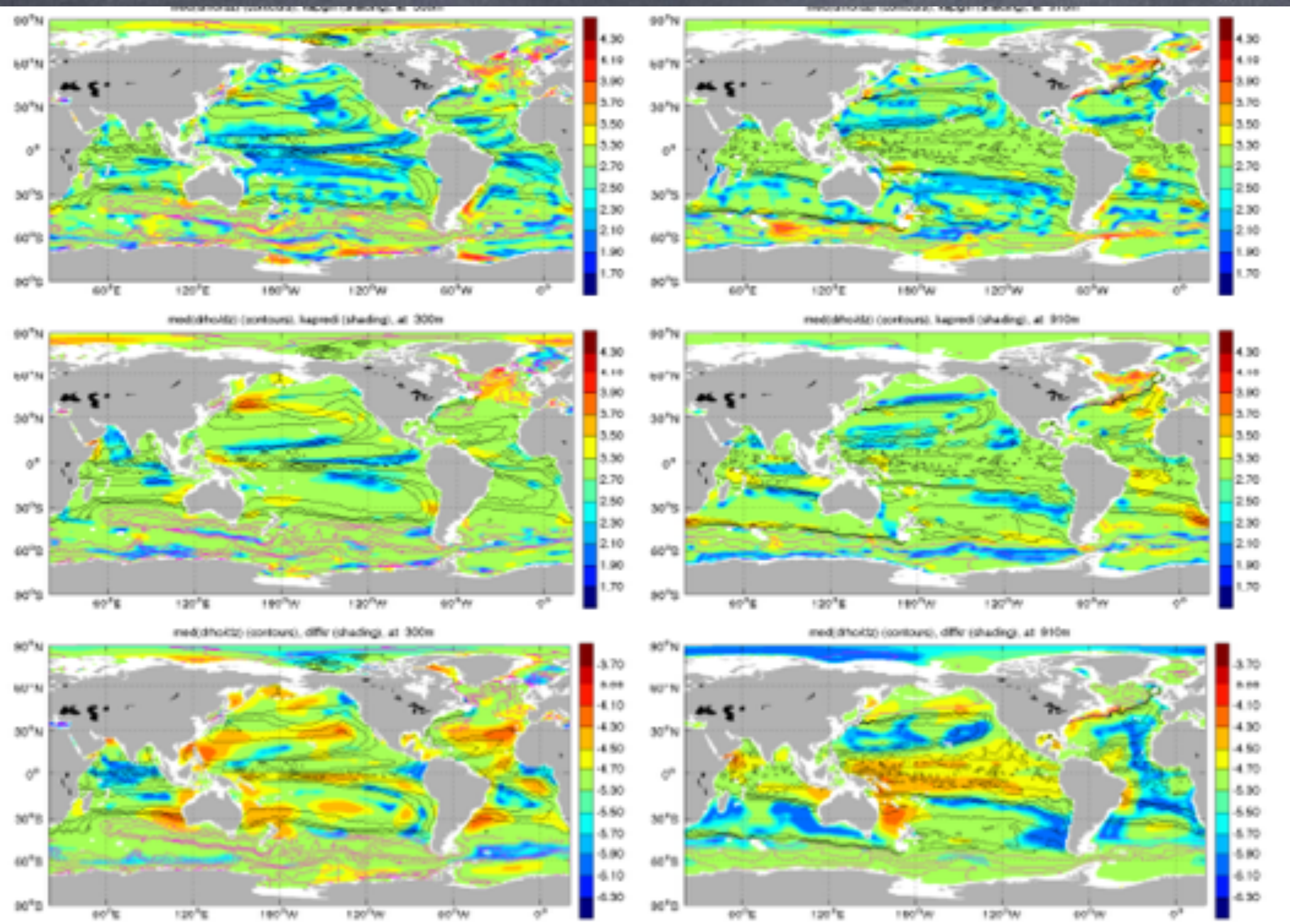

Figure 2: Estimated GM intensity (top), isopycnal diffusivity (middle) and diapycnal diffusivity (bottom) at 300m depth (left) and 900m depth (right) in log of m^2s^{-1} color scale. The respective first guess values are 10^3, 10^3 and 10^{-5} m^2s^{-1}. Overlaid contours depict the observed vertical density gradient (shown in detail at 300m, in Fig.5, top left). Overlaid black contours (resp. magenta contours) denote the $60^{th}, 70^{th}, 80^{th}, 90^{th}$ (resp. $10^{th}, 20^{th}, 30^{th}, 40^{th}$) percentiles of the observed stratification map.

Adjoint model: a means to invert uncertain parameters

(2) theory and practice

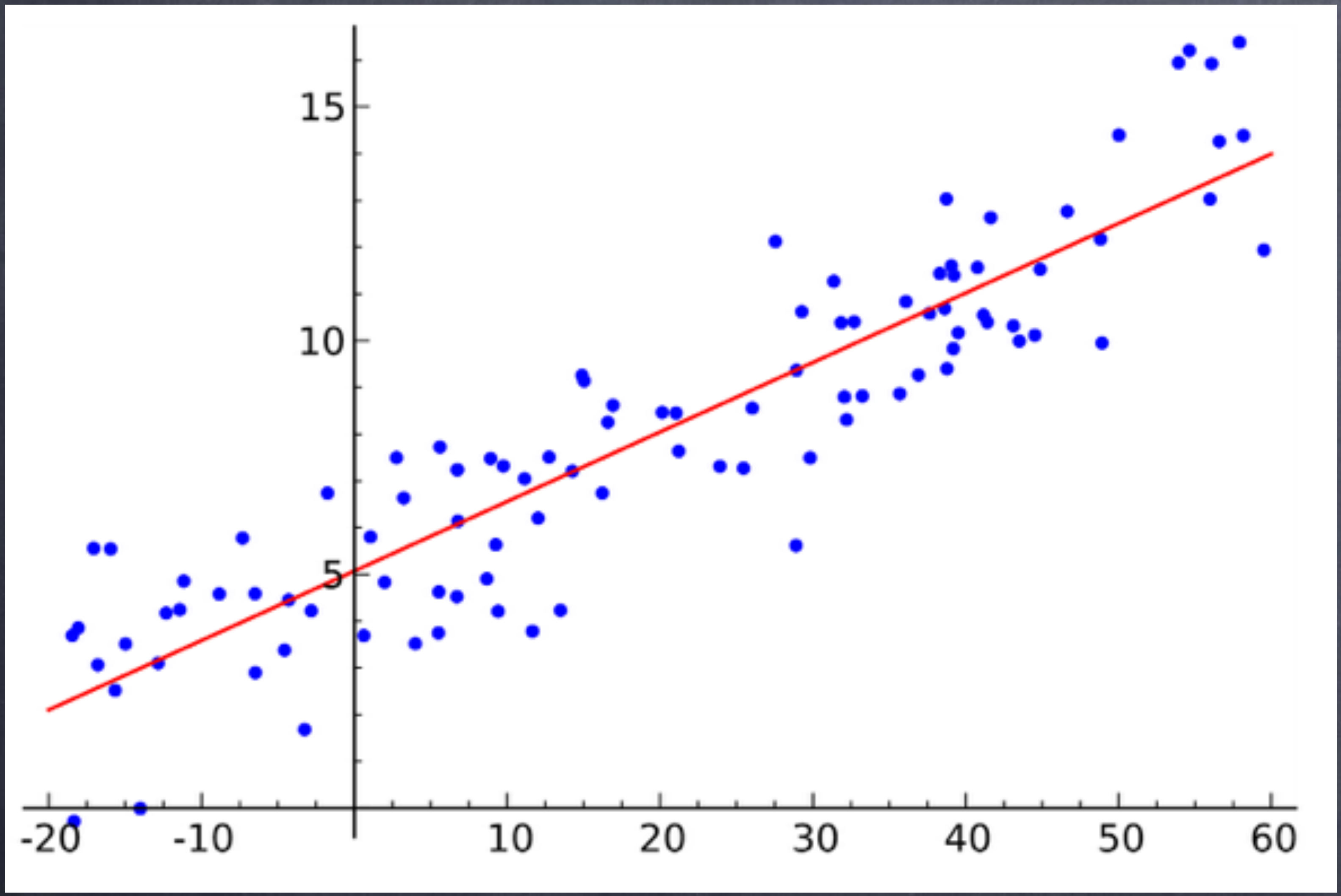

parameters, model
that best fit
observations

+

observational
uncertainty for
parameters, model

...

P(parameters, model | observations)

(2) theory and practice

$$x_n = D_n x_{n-1} + f_n \qquad n = 1, \cdots, N \tag{1}$$

forward model

$$J = \frac{1}{2} \sum_v [(\alpha_v - a_v)^T A_v (\alpha_v - a_v) + (\beta_v - b_v)^T B_v (\beta_v - b_v)] \tag{2}$$

least squares

$$L = J + \sum_{n=1}^{N} \lambda_n^T [x_n - D_n x_{n-1} - f_n] \tag{3}$$

Lagrange Mult.

$$x_n - D_n x_{n-1} - f_n = 0 \qquad n = 1, \cdots, N \tag{4c}$$

$$\lambda_n - D_{n_1}{}^* \lambda_{n+1} - \sum_v \frac{\partial a_v{}^T}{\partial x_n} A_v (\alpha_v - a_v) = 0 \quad n = 0, \cdots, N \tag{4d}$$

adjoint model

$$-\lambda_n - \sum_v \frac{\partial b_n{}^T}{\partial f_n} B_v (\beta_v - b_v) = 0 \qquad n = 1, \cdots, N \tag{4e}$$

(2) theory and practice

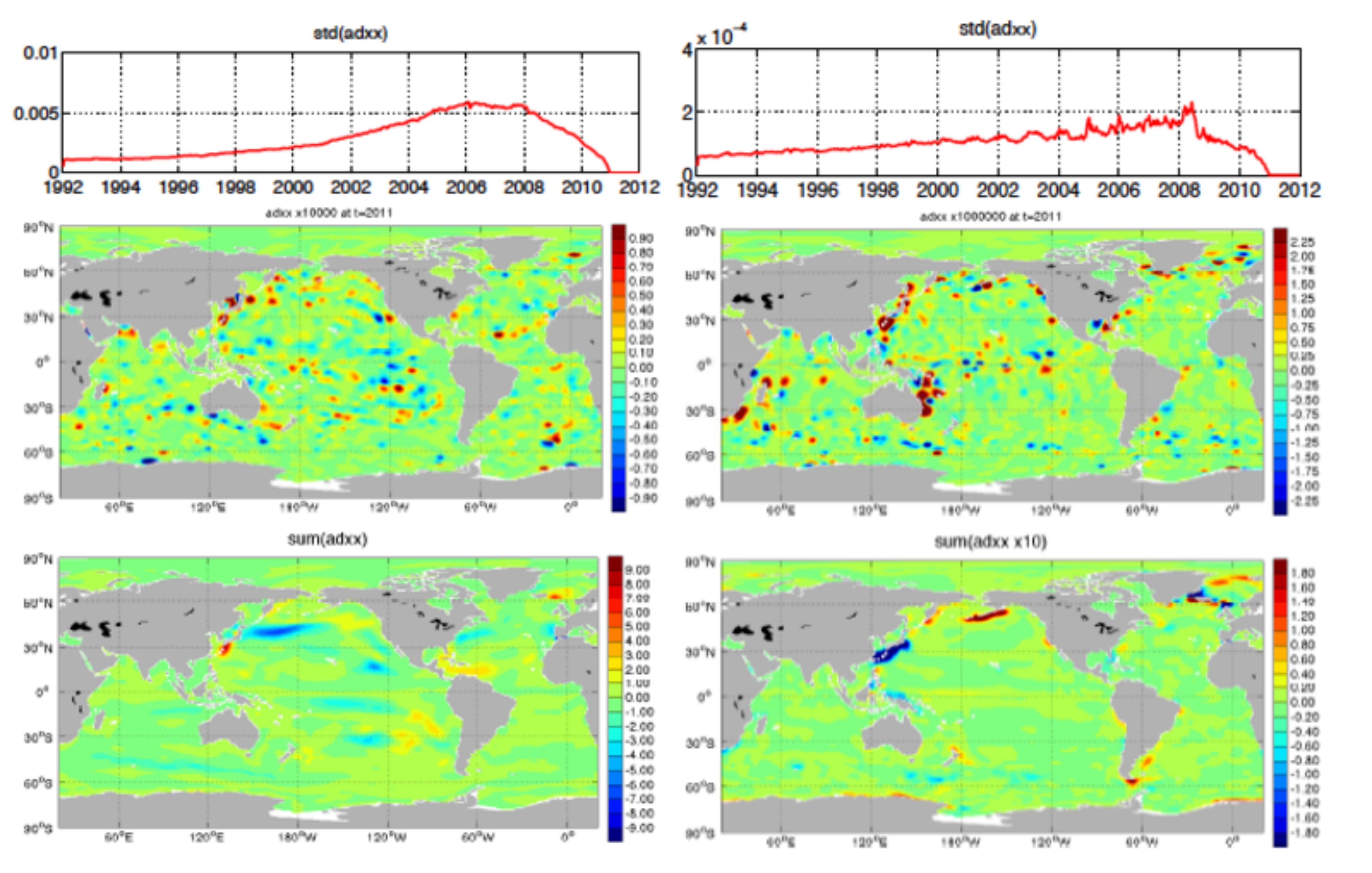

Adjoint model: MITgcm adjoint

(2) theory and practice

Fig. 10. Signal (left) and residual (right) for the barotropic streamfunction (upper; Eq. 2) and the meridional streamfunction (lower; Eq. 3), averaged over the last 6 months, in ARGOlike. Contour intervals: 4 Sv and 1 Sv respectively (1 Sv = 10^6 m^3 s^{-1}).

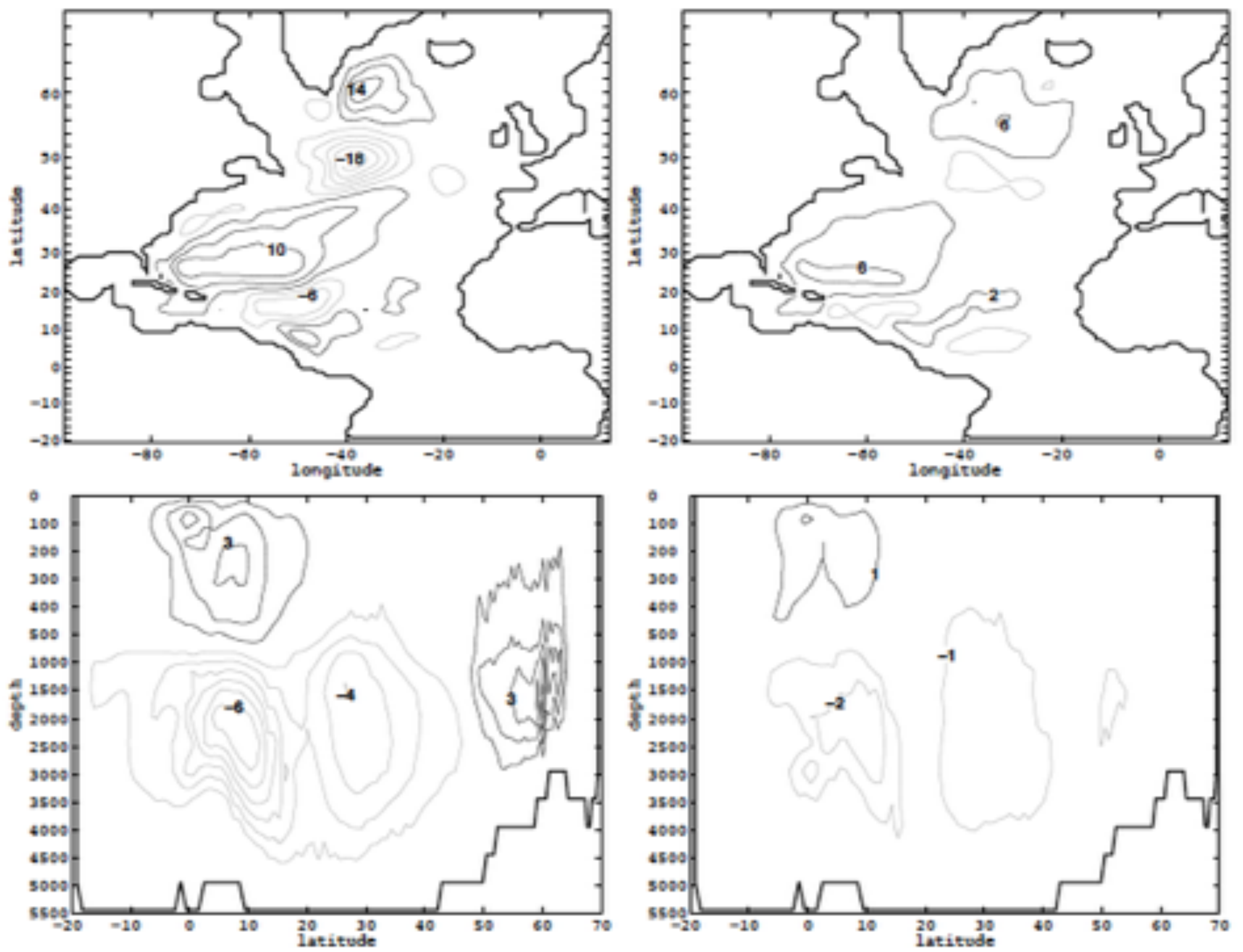

P(MOC | Argo) ????

(3) the ECCO v4 state estimate

period:
1992-2011

data constraints: $O(10^8)$
argo, altimetry, sst, etc.

model:
global, 1 degree, ocean+seaice, MITgcm

control parameters: $O(10^8)$
initial conditions, forcing, parametrized physics

… session #4

(3) the ECCO v4 state estimate

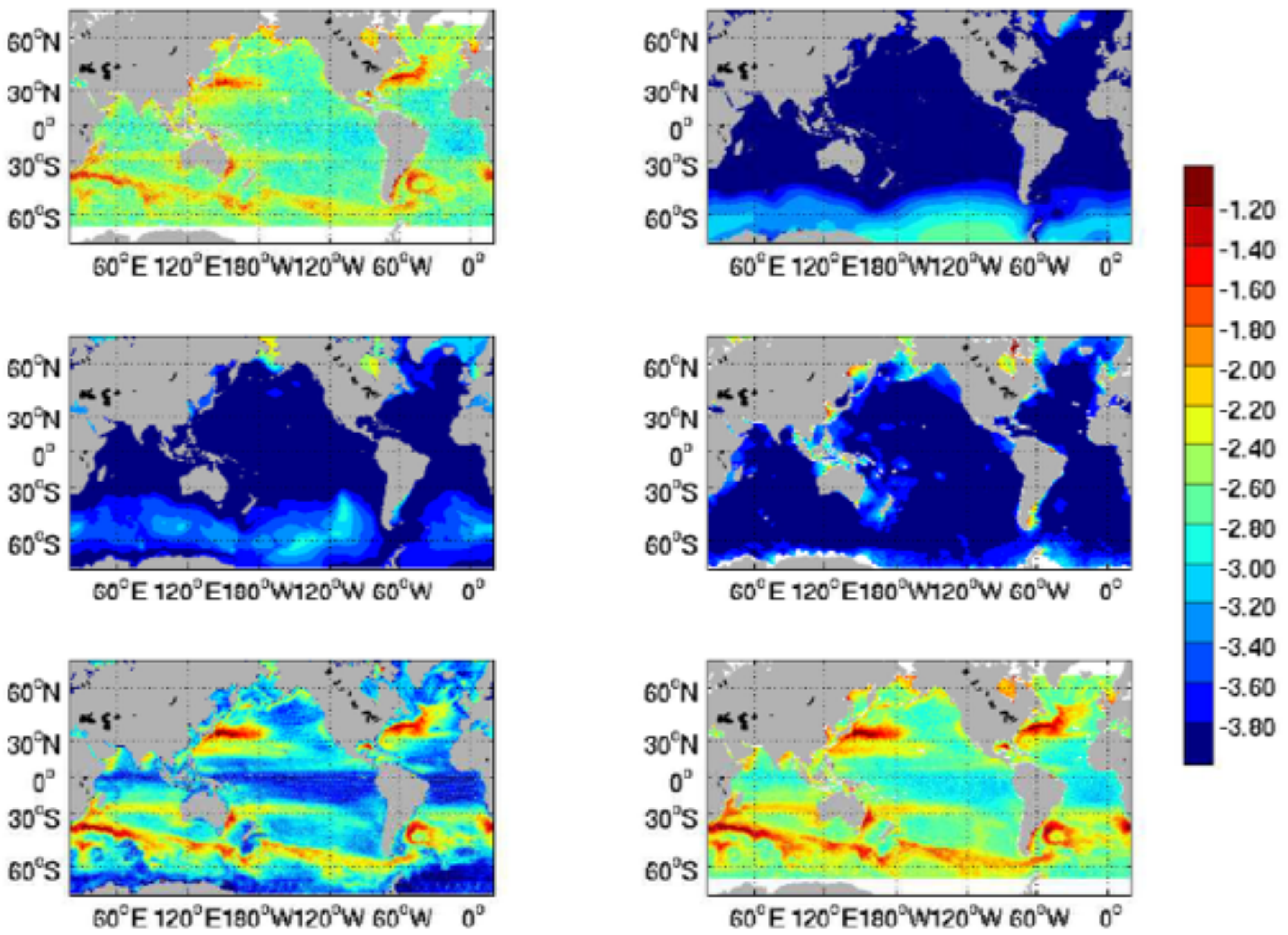

differences between Topex-Poseidon and ERS-Envisat over 1993-2010 (top left), differences in inverted barometer (IB) corrections calculated using ECMWF and NCEP pressure fields (top right), dynamic response to surface pressure forcing (middle left), differences between tide models (middle right) and meso-scale eddies (bottom left). The total error estimate ($\sigma^2_{a,pt}$; Eq 4) combining the 5 error contributions (see section 3.2 for details) is shown in the bottom right panel.

model-data errors:
altimetry example

(3) the ECCO v4 state estimate

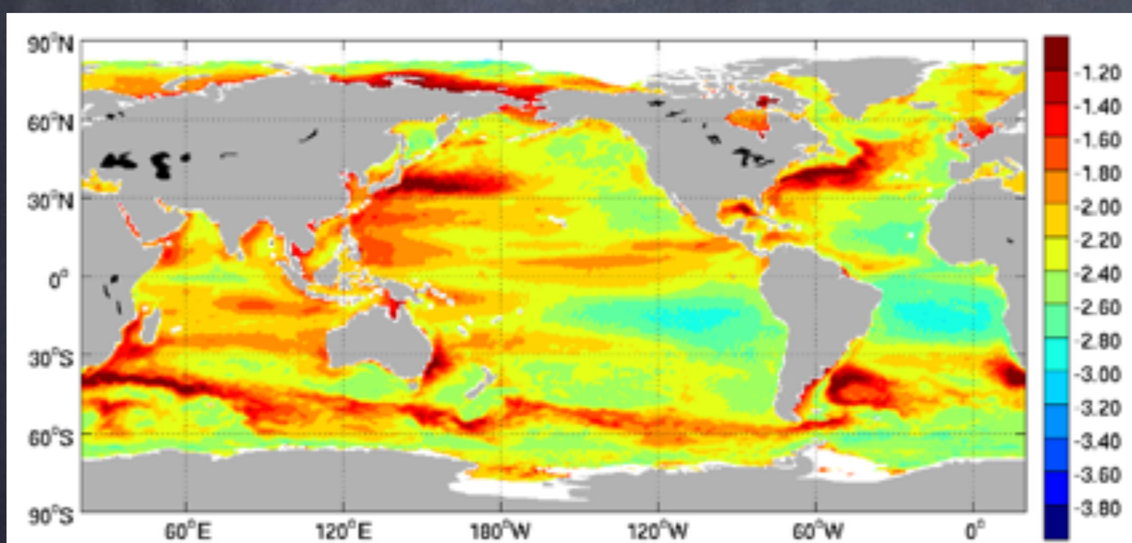

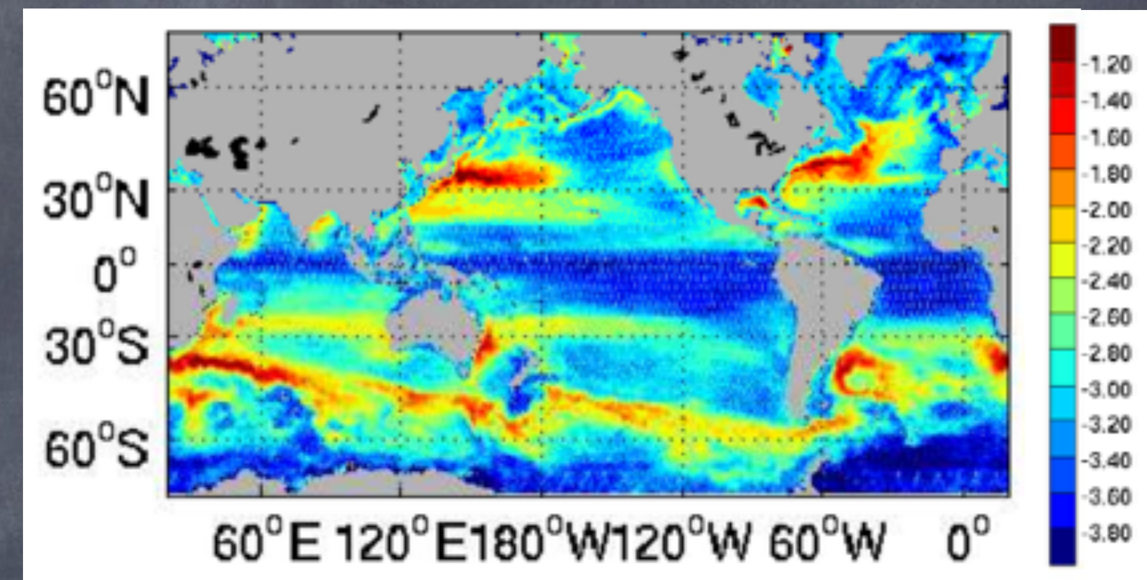

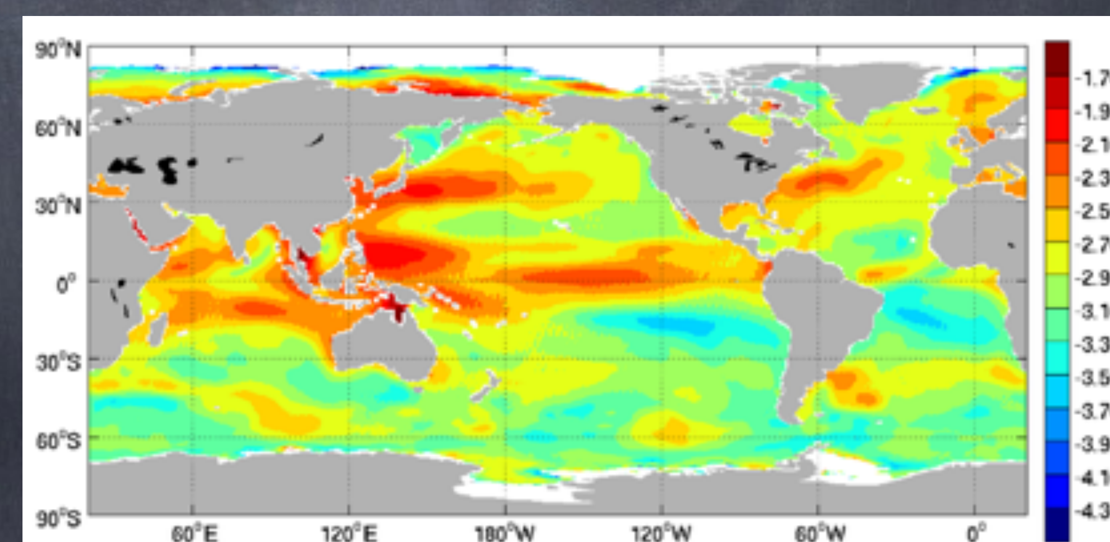

ECCO as a signal filtering problem: altimetry example

(3) the ECCO v4 state estimate

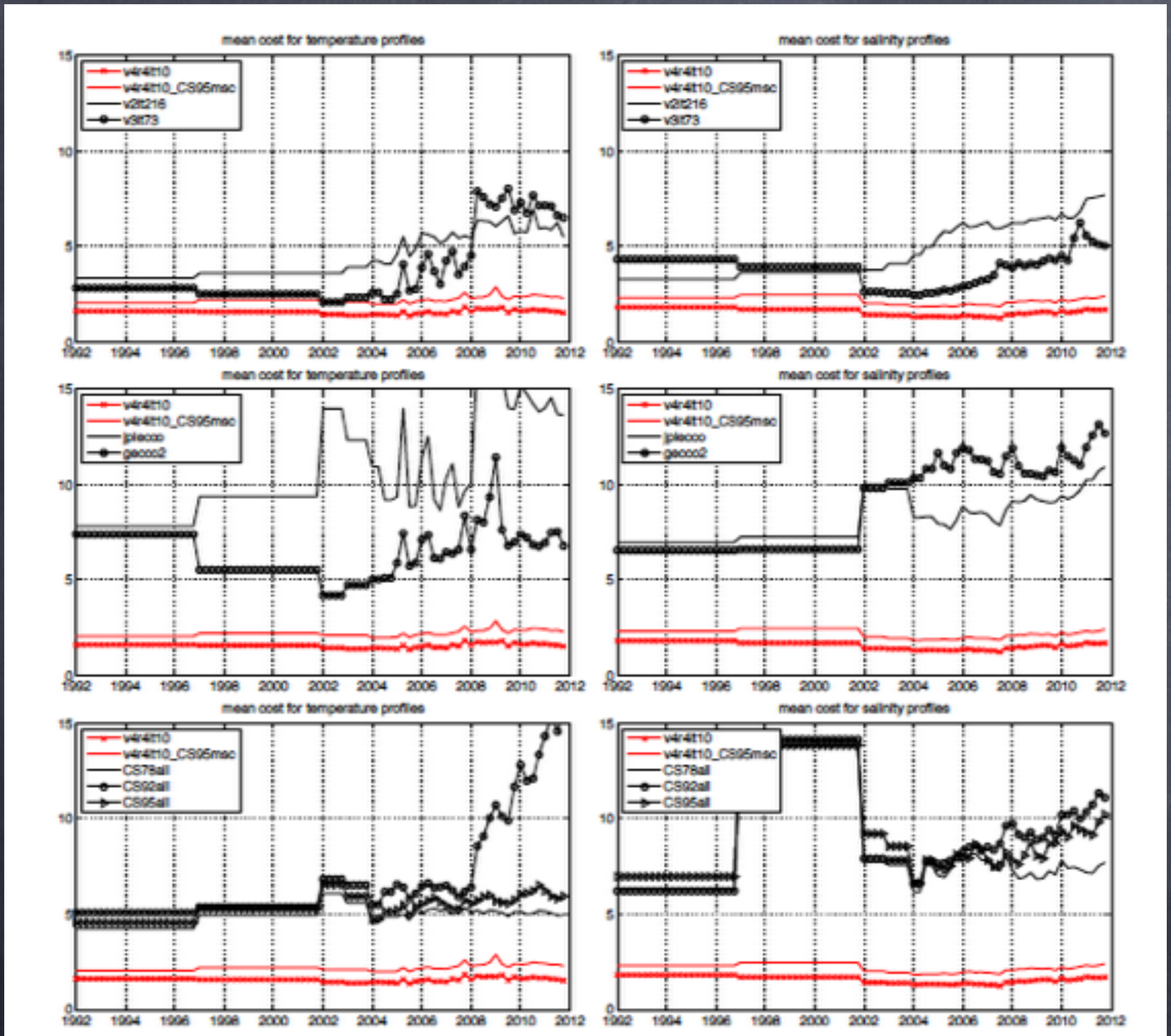

model data distance:

in situ data example

$$jT = (\text{prof\_Testim} - \text{prof\_T})^2 * \text{prof\_Tweight}$$
$$jS = (\text{prof\_Sestim} - \text{prof\_S})^2 * \text{prof\_Sweight}$$

using MITprof data, codes from class #1

(3) the ECCO v4 state estimate

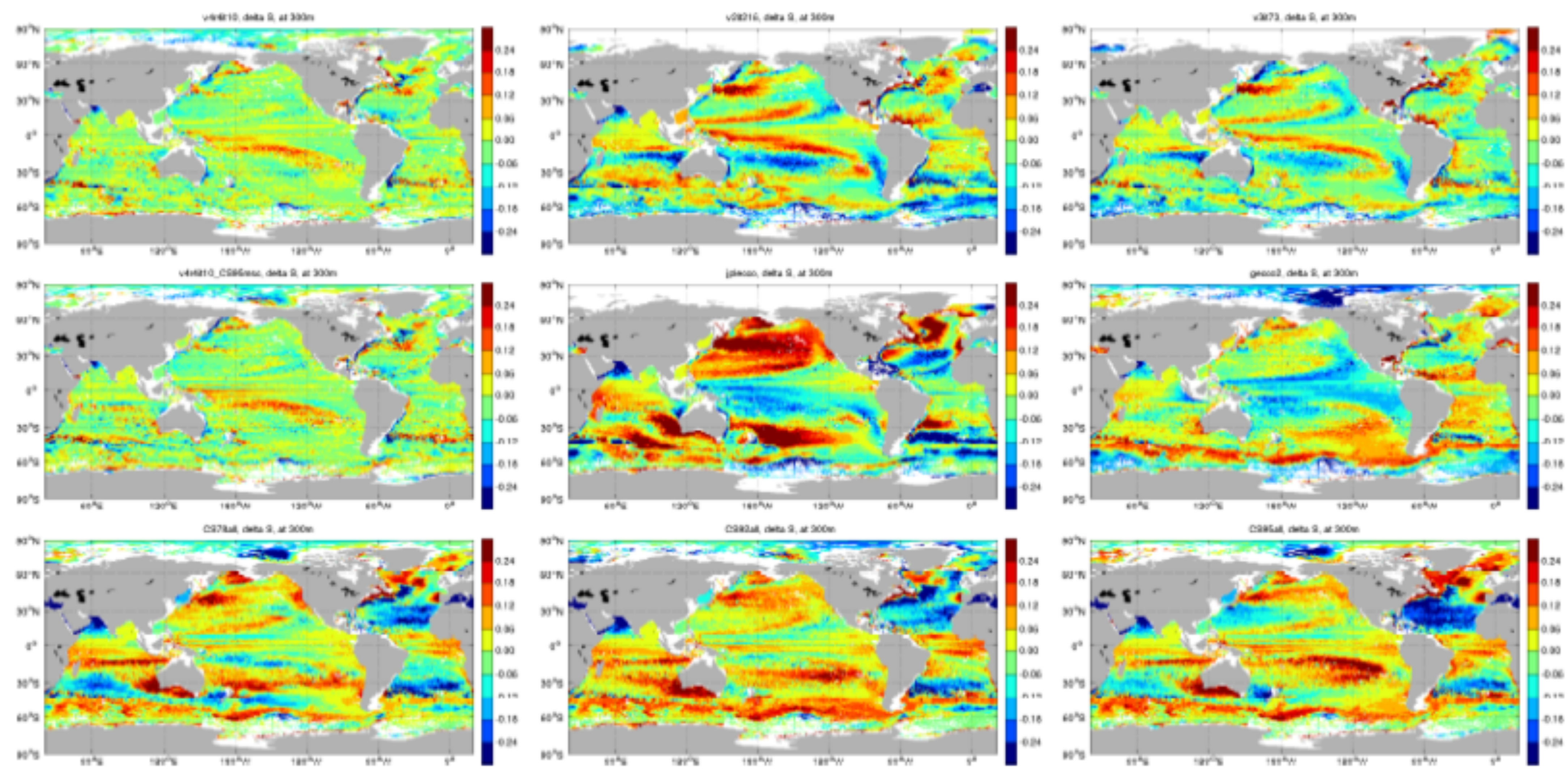

Figure 10: Model-data misfits for salinity at 300m depth computed by sample average (computational details are reported in the Fig.9 caption). ECCO v4 is depicted in the top left panel.

ECCO v4: reduced hydrography biases

(3) the ECCO v4 state estimate

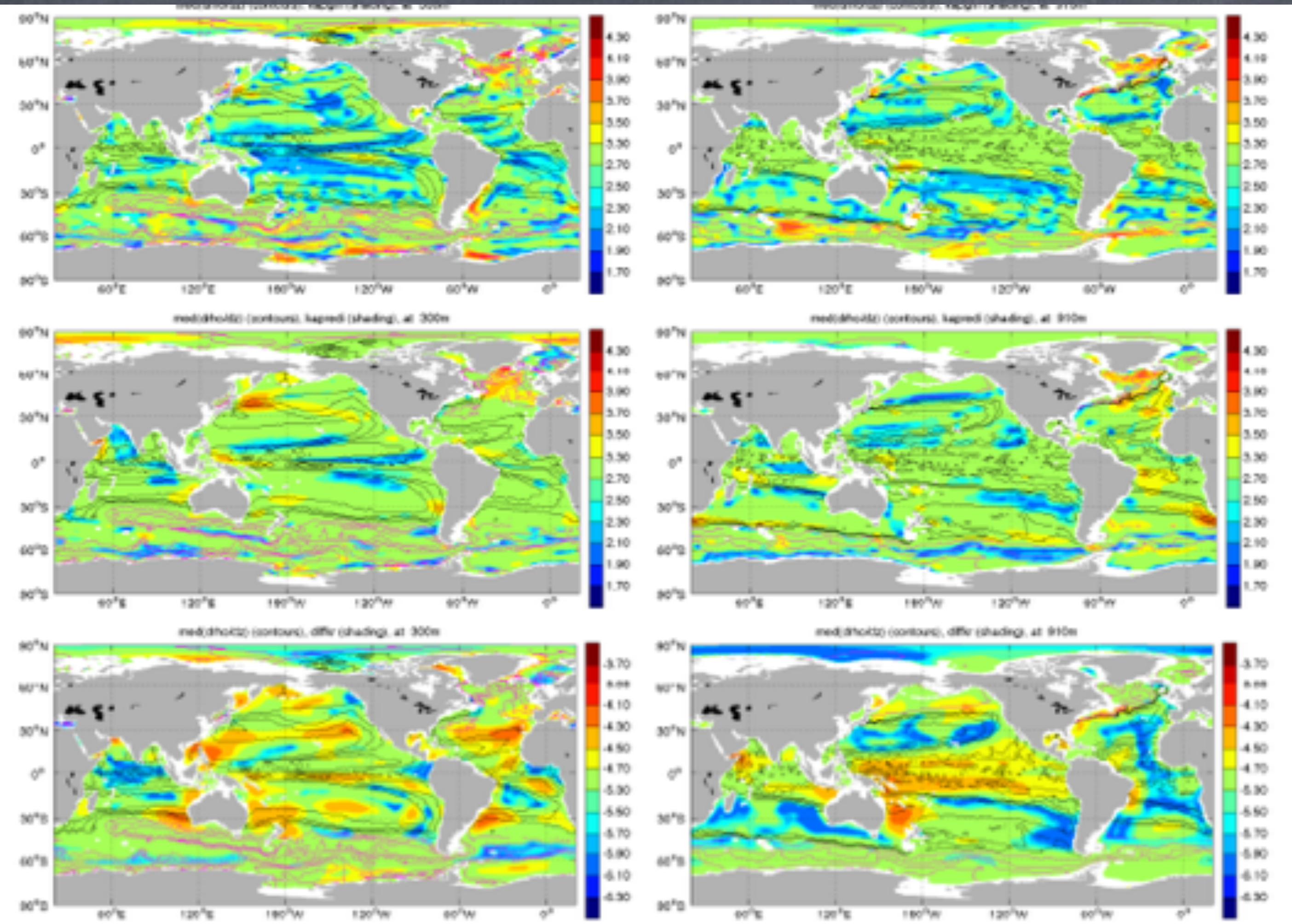

Figure 2: Estimated GM intensity (top), isopycnal diffusivity (middle) and diapycnal diffusivity (bottom) at 300m depth (left) and 900m depth (right) in log of m^2s^{-1} color scale. The respective first guess values are 10^3, 10^3 and 10^{-5} m^2s^{-1}. Overlaid contours depict the observed vertical density gradient (shown in detail at 300m, in Fig.5, top left). Overlaid black contours (resp. magenta contours) denote the $60^{th}, 70^{th}, 80^{th}, 90^{th}$ (resp. $10^{th}, 20^{th}, 30^{th}, 40^{th}$) percentiles of the observed stratification map.

ECCO v4: inverse parameter estimates

(4) extended model-data analyses

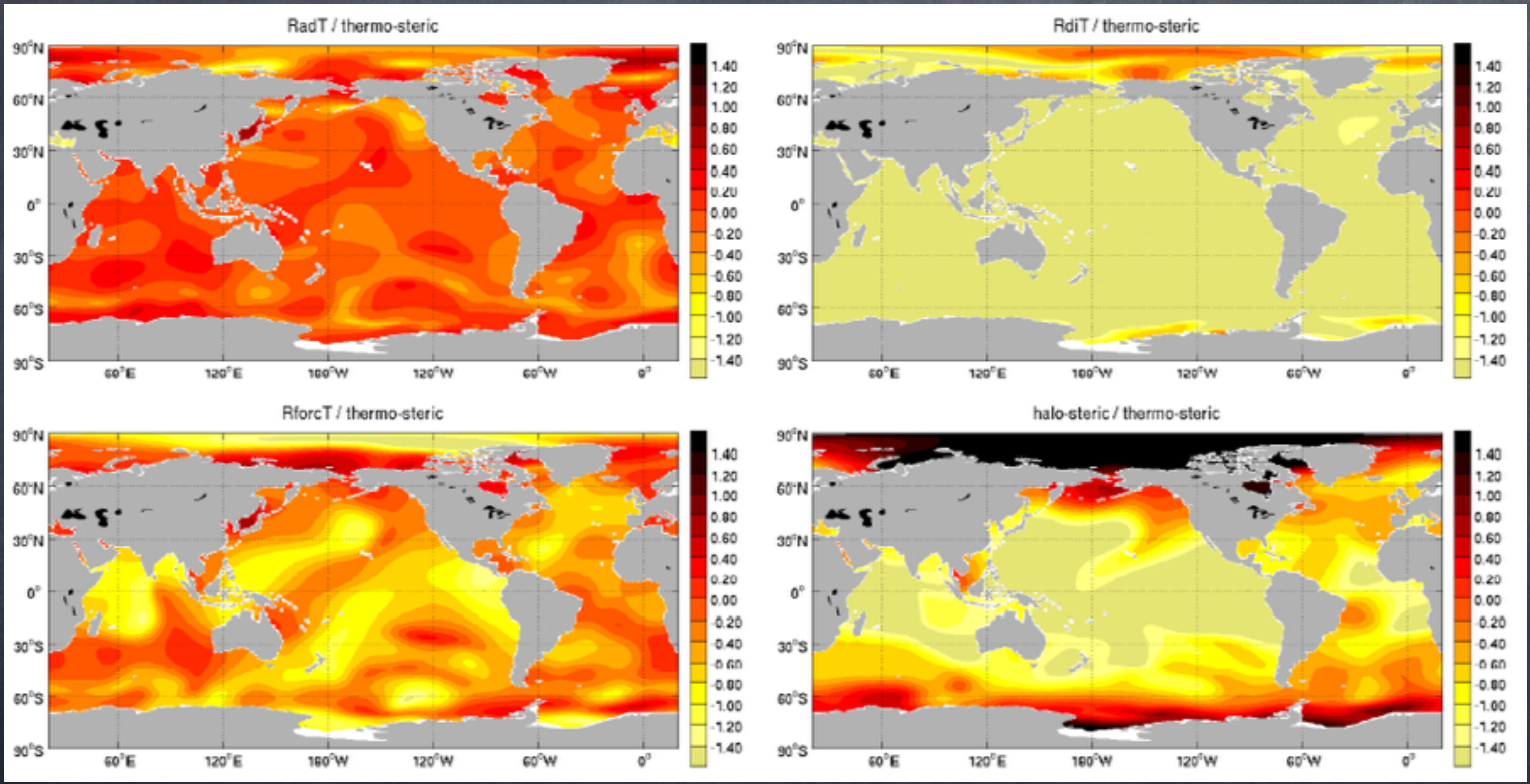

an altimetric example: budget of interannual variability

(4) extended model-data analyses

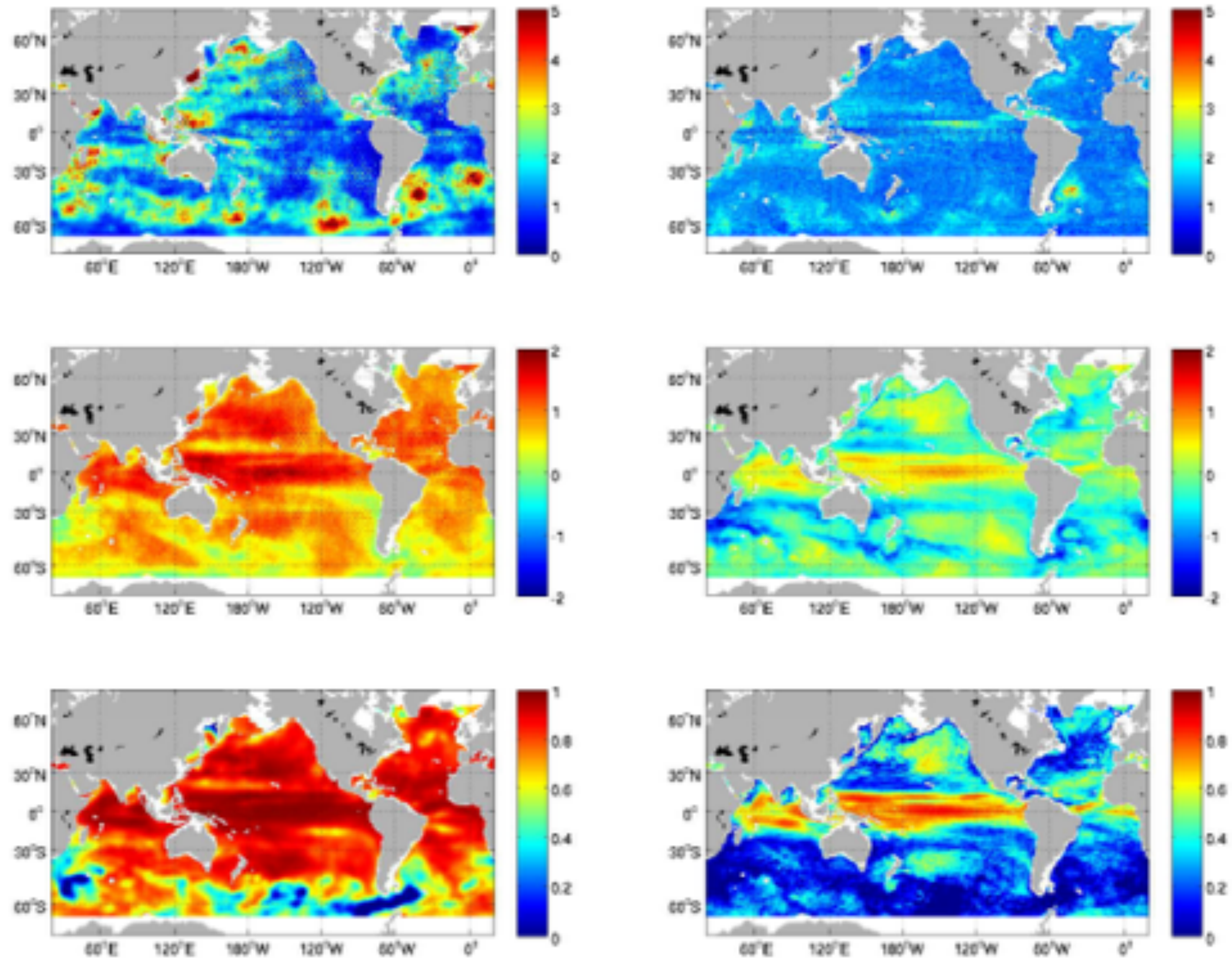

Figure 6: Assessment of the fit between the ECCO v4 state estimate and altimetry, for monthly large scale variability (left panels), and for pointwise daily variability (right panels). Top row: normalized model-data distance J_a, $J_{a,pt}$ (unitless; Eqs.2-3). Middle row: log of signal to noise ratio (unitless; Eq.6). Bottom row: R^2 coefficient of determination (unitless; Eq.7).

an altimetric example: model-data misfits

(4) extended model-data analyses

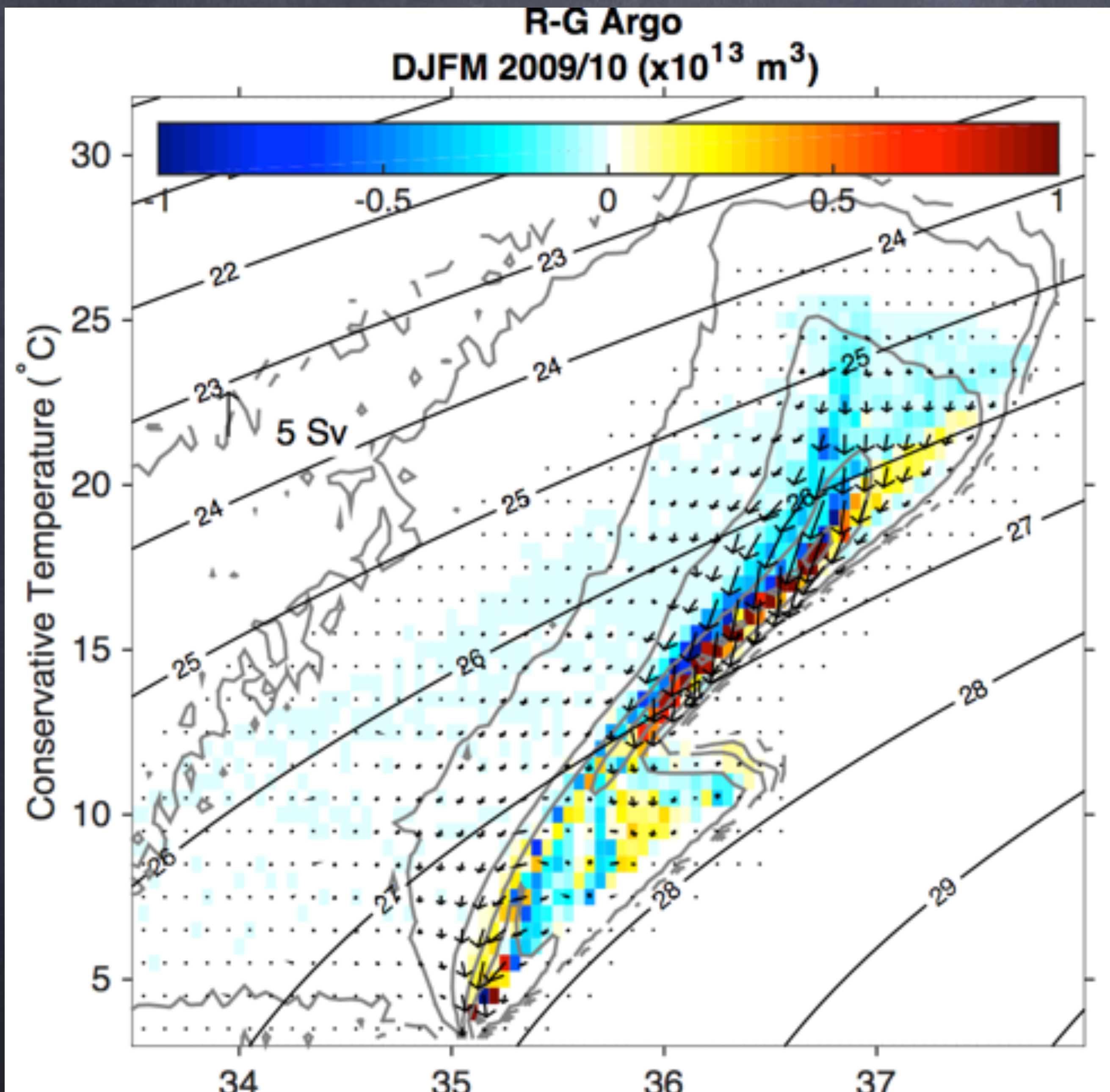

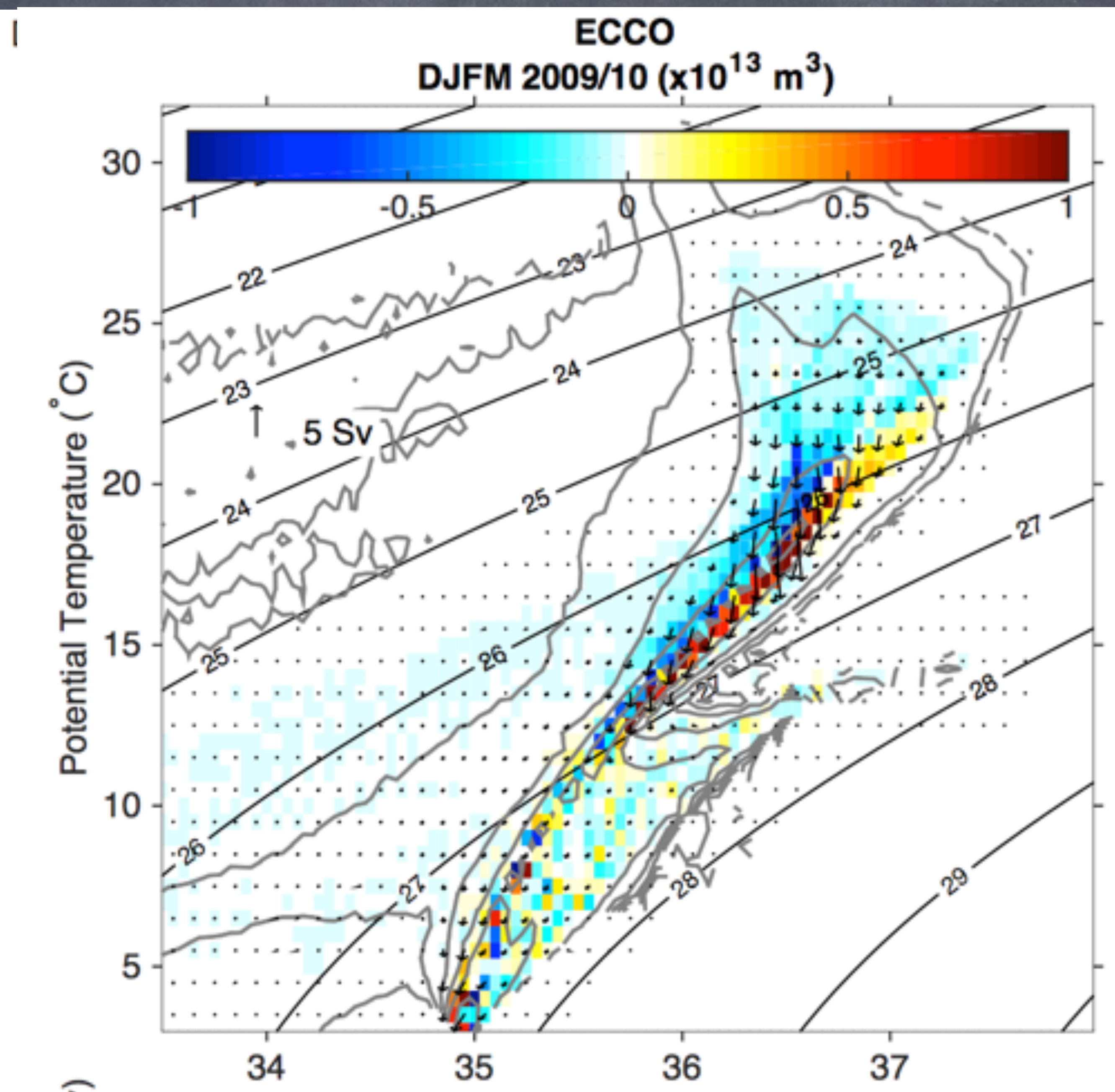

an hydrographic example: **water mass transformation**

(4) extended model-data analyses

summary of recent/ongoing analysis:

Speer and Forget 2013
Wunsch and Heimbach 2013, 2014,
Balmaseda et al. 2014,
Buckley et al. 2014, 2015,
Forget and Ponte 2015,
Forget 2015 a,b,
Forget et al 2015,
Fukumori et al. 2015,
Liang et al 2015 a,b,
Evans et al. 2015,
Chaudhuri et al. 2015

(5) interactive session : self-guided exercises

```
Below is a list of proposed, self guided exercises. I generally tried to order
the exercises by increasing complexity. While none of them is really challenging,
the various exercises aim to give you with first hand experience with the data sets
and tools discussed over the course of the IAP activity.

tips : - look for answers/examples in the programs we ran together in class #1 and #2
         - type 'help read_nctiles' in matlab and similarly for all other functions
         - use the matlab debugger to go through computations step by step
```

The actual listing is at

http://mitgcm.org/viewvc/*checkout*/MITgcm/MITgcm_contrib/gael/comm/course-idma2015/computing/iap-idma-exercises

(6) resources, bibliography

- Thacker and Long, 1988, Fitting dynamics to data
- Forget, 2010, Mapping ocean observations in a dynamical framework: A 2004-06 ocean atlas
- Forget and Ponte, under review, the Partition of Regional Sea Level Variability
- Forget, to be subm., On the observability of turbulent transport rates by Argo: evidence from an inversion experiment.
- Forget et al, to be subm., ECCO version 4: an integrated framework for non-linear inverse modeling and global ocean state estimation
- Forget et al, 2008, Combining Argo profiles with a general circulation model in the North Atlantic. Part 1: Estimation of hydrographic and circulation anomalies from synthetic profiles, over a year.
- Evans et al, in prep., Water mass variability in the Atlantic Subtropical Gyre reveals the mechanisms of recent Meridional Overturning changes.

(6) resources, bibliography

- Speer and Forget, 2013, Global Distribution and Formation of Mode Waters
- Wunsch and Heimbach, 2013, Two decades of the Atlantic meridional overturning circulation: Anatomy, variations, extremes, prediction, and overcoming its limitations.
- Wunsch and Heimbach, 2014, Bidecadal Thermal Changes in the Abyssal Ocean.
- Balmaseda et al, 2014, The Ocean Reanalyses Intercomparison Project (ORA-IP).
- Buckley et al, 2014, Low-frequency SST and upper-ocean heat content variability in the North Atlantic.
- Buckley et al, under review, Determining the origins of advective heat transport convergence variability in the North Atlantic.
- Forget, to be subm., The observed abyssal variability puzzle.
- Fukumori et al, under review, A Near-Uniform Fluctuation of Ocean Bottom Pressure and Sea Level across the Deep Ocean Basins of the Arctic Ocean and the Nordic Seas.
- Liang et al, under review, Vertical Redistribution of Oceanic Heat Content.
- Chaudhuri et al, in prep, Impact of uncertainties in atmospheric boundary conditions on ocean model solutions.